Supporting Information

Prediction of pH in multiphase multicomponent systems with ePC-SAFT advanced: Theory and Examples

Moreno Ascani, Daniel Pabsch, Marcel Klinksiek, Nicolás Gajardo-Parra, Gabriele Sadowski and Christoph Held*

Laboratory of Thermodynamics, Department of Biochemical and Chemical Engineering, TU Dortmund University, Emil-Figge-Str. 70, 44227 Dortmund, Germany.

E-mail: christoph.held@tu-dortmund.de

A. THERMODYNAMICS FUNDAMENTALS

Equilibrium Constant

Modeling of reaction equilibria requires the activity-based equilibrium constant K_a.

$$K_a(T, p) = K_x(T, p, x) \cdot K_\gamma(T, p, x) \prod_i (x_i \cdot \gamma_i)^{\nu_i} \tag{1}$$

For each reaction, the equilibrium constant can be expressed by the component's mole fractions x_i, thermodynamic activity coefficients γ_i , and stoichiometric coefficients ν_i (Eq. (1)). For the pH prediction, it is necessary to calculate the amount of H^+ in the mixture. K_x defines the mole-fraction based equilibrium constant and K_γ the activity coefficient based constant. K_a is independent of the composition in the liquid phase and only depends on temperature and pressure. The reactions considered in this work, for the system water-CO_2, are given as follows:

Involved reactions:	System:
$H_2O \rightleftharpoons OH^- + H^+$	
$H_2O + CO_2 \rightleftharpoons HCO_3^- + H^+$	Water-CO_2 (+salt)
$HCO_3^- \rightleftharpoons CO_3^{2-} + H^+$	
$H_2O \rightleftharpoons OH^- + H^+$	Water – solvent -acetic acid
$HAc \rightleftharpoons Ac^- + H^+$	
$H_2O \rightleftharpoons OH^- + H^+$	Water – solvent - oxalic acid
$HOx \rightleftharpoons Ox^- + H^+$ *(first dissociation)*	
$H_2O \rightleftharpoons OH^- + H^+$	Water – solvent - citric acid
$HCit \rightleftharpoons Cit^- + H^+$ *(first dissociation)*	

The activity coefficients γ_i were calculated via fugacity coefficients φ_i referred to the fugacity coefficient of the pure component φ_{0i} or referred to as an infinite diluted state φ_i^∞ according to Eq. (2-4).

$$\gamma_i^0 = \frac{\varphi_i(T, p, x)}{\varphi_{0i}(T, p, x_i = 1)} \tag{2}$$

$$\gamma_i^{*,x} = \frac{\varphi_i(T, p, x)}{\varphi_i^\infty(T, p, x_i = 0)} \tag{3}$$

$$\gamma_i^{*,\widetilde{m}} = \frac{\varphi_i(T, p, x)}{\varphi_i^\infty(T, p, x_i = 0)} x_w = \gamma_i^{*,x} x_w \tag{4}$$

The molality-based rational activity coefficient $\gamma_i^{*,\widetilde{m}}$ (Eq. (4)) is a very important quantity in electrolyte - and biothermodynamics and is used throughout this work to describe the non-ideality of all the dissolved species taking part in the reaction (Eq. (1)), except for water, for which the symmetric activity coefficient (Eq. (2)) is used. ePC-SAFT advanced is used in this work to describe the electrolyte system and calculate the fugacity coefficients.

Phase-equilibria calculations

In this work, a reactive flash calculation is employed to determine the species distribution and the pH of the aqueous phase in the investigated systems. At given conditions T and *p*, for an unimolar feed ($\sum_{i=1}^N N_i = \sum_{i=1}^N z_i = 1$) with composition z and a given, the goal is to find the number of phases π and composition set $\bar{\bar{x}} = \left(\bar{x}^{(1)}, \dots, \bar{x}^{(\pi)} \right)$ that minimizes the free energy G of the system. The number of stable phases at equilibrium and an estimation of their composition are determined by applying the tangent plane criterion of Michelsen[1,2] on the chemically equilibrated feed; however, no more than two phases were detected on the investigated systems, neither experimentally nor during modeling. After applying the tangent plane criterion, the obtained aqueous phase is further chemically equilibrated to improve the quality of the initial composition for the subsequent phase equilibrium calculation. The phase equilibrium calculation is accomplished by solving the system of equations given by Eq. (5) - (8).

$$1 - \frac{x_i^{(1)}}{x_i^{(2)}} exp\left(\ln \varphi_i^{(1)} - \ln \varphi_i^{(2)} \right) = 0 \qquad i \in \{1, \dots, N^{neu}\} \tag{5}$$

$$1 - \frac{x_{\pm,ij}^{(1)}}{x_{\pm,ij}^{(2)}} exp\left(\ln \varphi_{\pm,ij}^{(1)} - \ln \varphi_{\pm,ij}^{(2)} \right) = 0 \qquad i = cat, j = an \tag{6}$$

$$\left(N_i + \sum_{k=i}^{N^{reac}} \nu_{i,k} \lambda_k \right) - \sum_{j=1}^{\pi} n_i^{(j)} = 0 \qquad i = 1,.., N^{neu}, \ i = 1, \dots, N^{ch} - 1 \tag{7}$$

$$K_k - K_{x,k}^{(s)} K_{\gamma,k}^{(s)} = 0 \qquad\qquad k = 1, \dots, N^{reac} \tag{8}$$

In Eq. (5) - (8), N^{neu} denotes the number of neutral components, N^{ch} the number of charged components and N^{reac} the number of considered chemical reactions. λ_k is the reaction coordinate of the k-er chemical reaction and $\nu_{i,k}$ denotes the stoichiometric coefficient of component i in reaction j. The superscript (s) in Eq. (8) indicates a reference phase in which the equilibrium condition is imposed. In this work, the aqueous phase is always chosen to be the reference phase (It should be noticed that once Eq. (8) is fulfilled in one phase, due to equation (5) and (6) it is automatically fulfilled in all the other phases in which reactant and products of the reaction k are present). Furthermore, the presence of electrolytes is neglected in the vapor as well as in the organic phase because it is negligible in the investigated system. Therefore, the electrolytes are forced to remain in the aqueous phase, and Eq. (6) is neglected. The given system of equations is solved in an *inner loop* with a constant value of the fugacity coefficients $\ln \varphi_i^{(j)}$. The value of the fugacity coefficients is updated in an *outer loop*, and the system of equations is solved again until the change of the obtained solution after updating the fugacity coefficients is negligible.

ePC-SAFT advanced

Starting with the SAFT-based models developed by Chapman in 1989[3], significant progress in developing the equation of state based on perturbation theories was achieved. Gross and Sadowski first published PC-SAFT in 2001[4], which accounts for the perturbation of a hard chain instead of a hard-sphere. This framework was further developed in 2005 by Cameretti and Sadowski[5] to the electrolyte Perturbed-Chain Statistical Associating Fluid Theory (ePC-SAFT). ePC-SAFT includes electrostatic interionic interaction and, nowadays, a concentration-dependent dielectric constant[6]. Lately, the model was expanded with an altered Born term to include electrostatic interactions between charged components and their surrounding medium[7]. This enables the modeling of aqueous electrolyte solutions containing salts. The resulting 'ePC-SAFT advanced' model expresses the residual Helmholtz energy a^{res} is shown in Eq. (9).

$$a^{res} = a^{hc} + a^{disp} + a^{assoc} + a^{DH} + a^{born} \tag{9}$$

Here, a^{hc} is the respective energy contribution of the hard chain, a^{disp} and a^{assoc} describe the perturbations resulting from dispersive van der Waal attractions and hydrogen bonding. The analytical expressions of these three contributions are given in the original PC-SAFT publication[4]. In the presence of a charged species, the Debye-Hückel (DH) term a^{ion} is introduced to account Coulomb interactions. According to the theory of Debye and Hückel[8] ions are treated as spheres of a fixed diameter with a point charge in their center, immersed in a solvent considered[9] as a dielectric continuum of dielectric constant $\varepsilon = \varepsilon_0 \varepsilon_r$. The Debye-Hückel term is given in Eq. (10)

$$a^{ion} = -\frac{\kappa}{12\pi \cdot \varepsilon} \sum_j \chi_j q_j^2 x_j \tag{10}$$

Expression for the screening length (κ) and the "chi"-parameter (χ_j) are given elsewhere[5]. The Born contribution to the residual Helmholtz energy a^{Born} account the electrostatic interaction between ions and the surrounding solvent solvation model and is expressed by Eq. (10) [7].

$$a^{Born} = -\frac{e^2}{4\pi\varepsilon_0 k_B T}\left(1 - \frac{1}{\varepsilon_r}\right)\sum_r \frac{z_i^2 x_i}{a_i} \tag{11}$$

In Eq. (11) e describe the elementary charge and the Born radii a_i were set to the respective diameters of the ions estimated within the original ePC-SAFT. Further information about the DH

and Born term is given in the literature [7]. "ePC-SAFT advanced" requires five pure-component parameters for each associating component i. These parameters are the segment number m_i^{seg}, segment diameter σ_i, the dispersion-energy parameter u_i/k_B, the association-energy parameter ε^{AiBi} and association-volume parameter κ^{AiBi}. For associating components an association scheme needs to be defined. For water the 2B model was used[10].

Additionally, one binary interaction parameter k_{ij} between two components, i and j, as well as the dielectric constant of the pure component, is required. For the calculation of mixture properties combining rules of Berthelot-Lorenz are applied Eq. (12) and (13):

$$\sigma_{ij} = \frac{1}{2}(\sigma_i + \sigma_j) \tag{12}$$

$$u_{ij} = \sqrt{u_i u_j}(1 - k_{ij}) \tag{13}$$

ePC-SAFT advanced modeling results were compared to experimental data. For that purpose, the average absolute relative deviation (*AARD*) related to the mean value of experimental solubility data (Eq. 14)) was used.

$$ARD(\%) = 100 \times \frac{N_{exp} - N_{PC-SAFT}}{N_{exp}} \tag{14}$$

Where N_{exp} denotes literature data and $N_{PC-SAFT}$ represents the results from ePC-SAFT advanced. The calculated ARD values for the investigated systems are listed and evaluated in Table S6.

B. SUPPORTING FIGURES
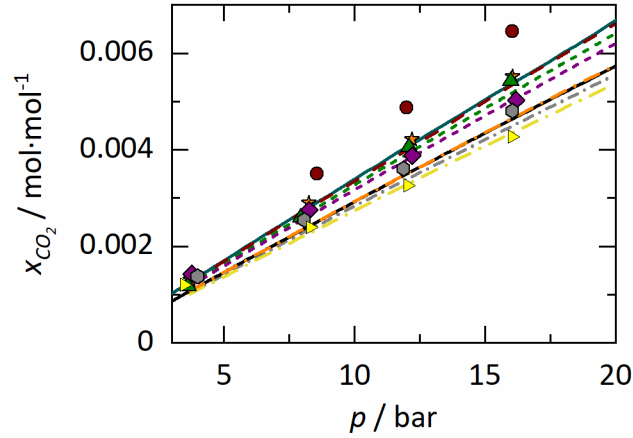
Figure S1: Vapor liquid equilibrium from the systems water + CO_2 + $NaHCO_3$. T= 313 K and m̃ = 0.1 mol/kg, (circles), T= 313 K and m̃ = 0.5 mol/kg, (stars), T= 323 K and m̃ = 0.1 mol/kg (triangles), T= 313 K and m̃ = 1 mol/kg (diamond), T= 323 K and m̃ = 0.5 mol/kg (hexagon) and T= 323 K and m̃ = 1 mol/kg (right-point triangle). Dashed lines represente ePC-SAFT , and continuous line represents ePC-SAFT using parameters from Table S1, S2 and S3.
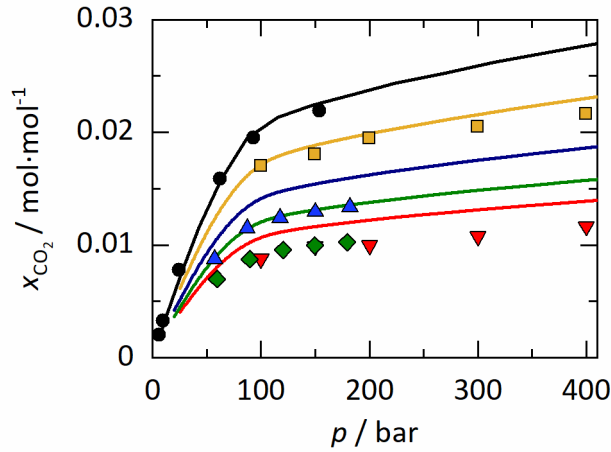
Figure S2: CO_2 mole fraction solubility as a function of pressure at T =323 K for different NaCl molalities (circles salt free from Peng et al.[11] squares m̃ = 1 mol/kg , and down-triangles m̃ = 5 mol/kg from Yan et al.[12], up-triangles m̃ = 2.5 mol/kg and diamonds m̃ = 4 mol/kg from Hou et al.[13]). Lines are ePC- SAFT modeling results using parameters from Tables S1-S3.
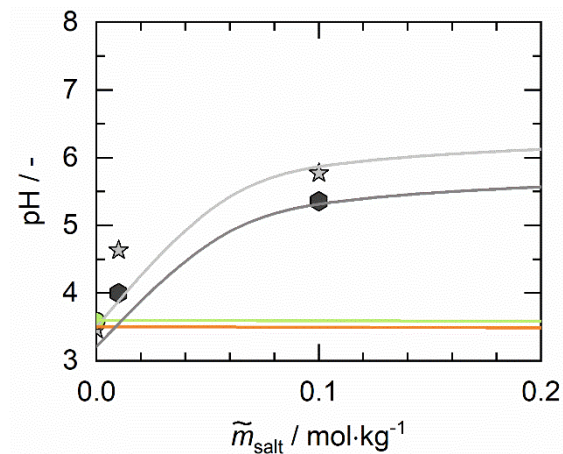
Figure S3: *pH* of the ternary system CO_2 + water + salt as a function of salt molality $\tilde{m}_{salt}$ at equilibrium CO_2 concentrations. Symbols are experimental data from the literature (stars[11]: $NaHCO_3$ at $T = 308$ K and $p = 9.2$ bar, hexagons[11]: $NaHCO_3$ at $T = 308$ K and $p = 43$ bar, circles[11]: NaCl $T = 343$ K and $p = 10$ bar, and triangles[14]: KCl at $T = 298$ K and $p = 9$ bar). Lines are ePC- SAFT modeling results using parameters from Tables S1-S3.
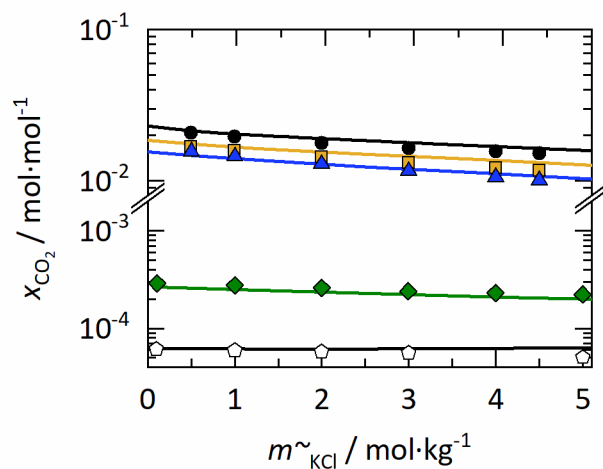
Figure S4: CO_2 mole fraction solubility as a function of KCl molality at different pressures (150 bar from Zhao et al.[15]: circles T = 323 K, squares T = 373 K, and up-triangles T =423 K; 1 bar from He et al.[16]: diamond T = 323 K and pentagons T = 363 K). Lines: ePC-SAFT modeling results using parameters from Tables S1-S3.
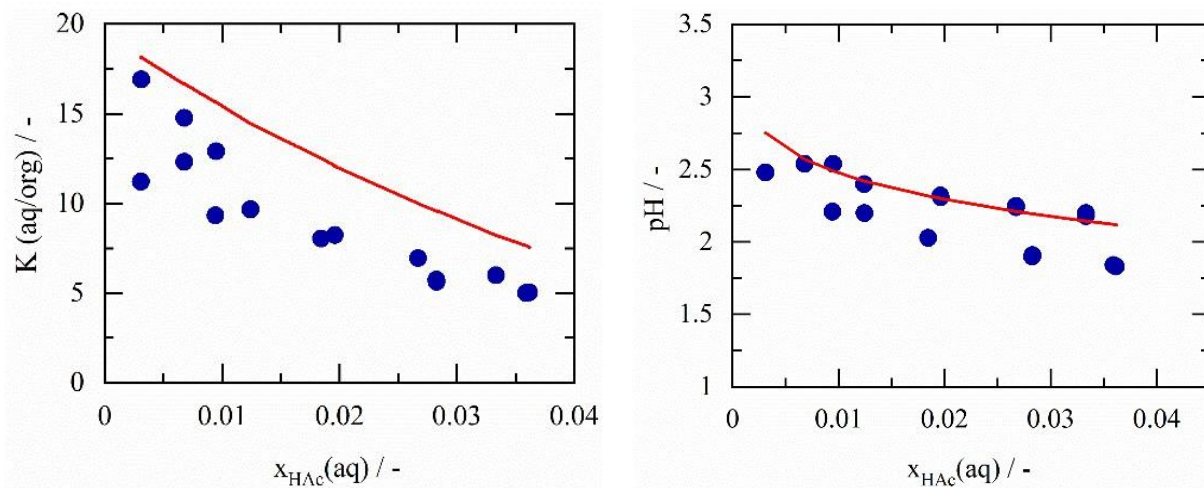
Figure S5: Partition coefficient of acetic acid in the mixture of water and toluene. Blue circles represent experimental literature data from Kirsch et al.[17] compared to modeling results obtained with the ePC-SAFT (red line) using parameters from Table S1, S2 and S3.

C. SUPPORTING TABLES

Table 1: Pure-component parameters of water and the organic solvents used in this work.

Solvent	m_i^{seg}	σ_i / Å	u_i/k_B / K	N:N	ε^{AiBi} / K	κ^{AiBi}	Ref.
Water	1.2047	2.7927	353.95	1:1	2425.7	0.04510	[18]
CO_2	2.0729	2.7852	169.21	1:1	0	0.04510	[19]
MIBK	3.6799	3.3628	259.89	1:1	-	0.04510	[20]
Toluene	2.8149	3.7169	285.69	-	-	-	[4]
Acetic Acid	1.3403	3.8582	211.59	1:1	3044.4	0.07555	[21]
Oxalic acid	3.3585	2.7486	180.14	1:1	1654.78	0.02000	[22]
Citric acid	8.546	2.723	227.18	4:4	2488	0.044	[23]

Table 2: ePC-SAFT pure-component parameters.[24] Segment number is unity for all ions. For the oxalate anion, the same pure-component parameters as for oxalic acid were used and a negative charged segment was added. Binary interaction parameters k_{ij} between water and ions were all set to zero.

Ion	σ_i / Å	u_i/k_B / K
Na^+	2.8232	230.00
K^+	3.3417	200.00
Cl^-	2.7560	170.00
HCO_3^-	2.9296	70.00
CO_3^{2-}	2.4422	249.26
H^+	3.4656	500.00
OH^-	2.0177	650.00
Ac^-	3.9328	150.00
Ci^-	4.4600	250.00

Table 3: Binary interaction parameters used in this work.

Binary systems	$k_{ij,a}$	$k_{ij,T}$	Ref.
Water-CO_2	0.0122	0.0003016	19
Na^+ - HCO_3^-	-0.51400	-	24
K^+ - Cl^-	0.064	-	24
Na^+ - Cl^-	0.317	-	24
H^+ - Cl^-	0.654	-	24
Na^+ - OH^-	0.649	-	24
K^+ - OH^-	1.000	-	24
Water - Toluene	0.02100	0.000726	24
Water - Acetic acid	-0.12470	-	25
Water - MIBK	-0.0550	-	26
Water – Oxalic acid	-0.02560	-	22
Water – Citric acid	-0.11000	-	27
Toluene – Acetic acid	-0.08317	-	This work
MIBK – Oxalic acid	0.16300	-	This work
MIBK – Citric acid	-0.25000	-	This work

Table 4: pKa values of the acids used in this work. Temperature- and pressure-dependent correlations, whenever used, are denoted in the table by a "f(T,p)" and can be found in the respective references.

Acid	pK_a	Ref.
Acetic acid	4.76	28
Oxalic acid	1.23	29
Citric Acid	3.13	28
Water (autoprotolysis)	f(T,p)	30,31
CO_2	f(T,p)	30,31

HCO_3^-	f(T,p)	[30,31]

Table 5: Dielectric constants for solvents and salts applied in this work. All salts are modeled with a similar dielectric constant that is a mean of available experimental data.

Component	Dielectric constant / $C \cdot Vm^{-1}$	Ref.
Water	$-105.2 \ln T + 677.480$	[32]
Salts	8	a)

a) All salts were modeled with the same dielectric constant as the mean of available experimental data.[33]

Table 6: Compared literature data for the investigated system and the corresponding AARD.

System	Data points	T and p range	AARD %
CO_2 / Water	37	308 – 413 K 20 – 153 bar	1.339
CO_2 / Water / $NaHCO_3$	29	308 – 353 K 10 – 153 bar	5.187
CO_2 / Water / NaCl	3	343 K 10 bar	1.952
CO_2 / Water / KCl	2	298 K 9 bar	0.833
Toluene / Water / Acetic Acid	19	298 K 1 bar	6.902
MIBK / Water / Oxalic Acid	19	298 K 1 bar	9.690
MIBK / Water / Citric Acid	9	298 K 1 bar	43.436

Table 7: Literature data and modeling results obtained with ePC-SAFT advanced for the binary system CO_2 + water. *Literature data taken from Peng et al.[34].

T / K	p / bar	pH$^{exp.,*}$ / -	pH^{Modeled} / -	ARD / %
308.3	3.8	3.71	3.701	0.243
	6.1	3.58	3.613	0.922
	9.7	3.46	3.525	1.879
	24.3	3.22	3.314	2.919

	62.3	3.05	3.143	3.049
	92.8	3.01	3.102	3.056
	153.8	2.97	3.072	3.434
323	3.8	3.76	3.737	0.612
	6.1	3.63	3.647	0.468
	9.8	3.52	3.536	0.455
	24.3	3.36	3.347	0.387
	62.3	3.14	3.173	1.051
	92.8	3.07	3.112	1.368
	153.6	3.04	3.070	0.987
343	3.8	3.89	3.81	2.057
	6.1	3.72	3.71	0.269
	9.9	3.59	3.60	0.279
	24.3	3.42	3.41	0.292
	62.2	3.25	3.23	0.615
	92.8	3.18	3.16	0.629
	153.9	3.12	3.09	0.962
368.1	6	3.97	3.827	3.602
	10	3.77	3.704	1.751
	24.2	3.56	3.502	1.629
	63.6	3.35	3.316	1.015
	93	3.28	3.240	1.220
	154.1	3.23	3.154	2.353
398.3	10	3.97	3.875	2.393
	24.4	3.63	3.647	0.468
	62.9	3.47	3.447	0.663
	93.6	3.34	3.364	0.719
	153.6	3.32	3.269	1.536
423.2	10	4.11	4.083	0.657
	24.4	3.78	3.794	0.370
	62.9	3.59	3.574	0.446

| | 93.6 | | 3.54 | 3.484 | 1.582 |
| | 153.7 | | 3.49 | 3.378 | 3.209 |

Table 8: Literature data and modeling results obtained with ePC-SAFT advanced for the system CO_2 + water + $NaHCO_3$. *Literature data taken from Li et al.[11] and Han et al [35].

T / K	p / bar	$\widetilde{m}_{salt}$ / mol·kg^{-1}	pH$^{exp.,*}$ / -	pH^{Modeled} / -	ARD / %
308.3	10	0	3.46	3.5	1.156
		0.01	4.63	4.3	7.127
		0.1	5.77	5.9	2.253
		1	6.99	6.8	2.718
	43.2	0.01	4	4.06	1.500
		0.1	5.36	5.259	1.884
		1	6.42	6.246	2.710
	153.5	0	2.97	3	1.010
		0.01	3.82	3.87	1.309
		0.1	5.23	5.12	2.103
		1	6.29	6.02	4.293
323	10	0.01	4.85	4.9	1.031
		0.1	5.9	5.95	0.847
		1	7.17	6.75	5.858
	43.2	0.01	4.2	3.2	23.810
		0.1	5.49	5.4	1.639
		1	6.54	6.29	3.823
	153.5	0.01	3.99	3.1	22.306
		0.1	5.35	5.1	4.673
		1	6.43	6.01	6.532
353	10	0.01	5.16	4.9	5.039
		0.1	6.29	6	4.610
		1	7.56	6.851	9.378
	43.2	0.01	4.44	4.2	5.405
		0.1	5.71	5.59	2.102
		1	6.93	6.42	7.359

153.5	0.01	4.15	4.1	1.205
	0.1	5.59	5.19	7.156
	1	6.68	6.04	9.581

Table 9: Literature data and modeling results obtained with ePC-SAFT advanced for the system CO_2 + water + NaCl. *Literature data taken from Li et al.[11]

T / K	p / bar	$\widetilde{m}_{salt}$ / mol·kg⁻¹	pH$^{exp.,*}$ / -	pH^{Modeled} / -	ARD / %
343	10	1	3.47	3.52	1.441
		3	3.42	3.418	0.058
		5	3.19	3.329	4.357

Table 10: Literature data and modeling results obtained with ePC-SAFT advanced for the system CO_2 + water + KCl. *Literature data taken from Mutailipu et al.[14]

T / K	p / bar	$\widetilde{m}_{salt}$ / mol·kg⁻¹	pH$^{exp.,*}$ / -	pH^{Modeled} / -	ARD / %
298	9	2	3.34	3.32	0.599
		4	3.19	3.156	1.066

Table 11: Literature data and modeling results of the partition coefficient for the system water + toluene + acetic acid. *Literature data taken from Ziegenfuß and Maurer[36].

$x_{Acetic\ acid}$ / mol·mol^{-1}	$K^{aq./org.,exp.,*}$ / mol·mol^{-1}	$K^{aq./org.,\ modeled}$ / mol·mol^{-1}	ARD / %
0.003106633	16.9139579	18.479	9.253
0.003088565	11.21141981	18.459	64.645
0.006780777	12.30590357	16.825	36.723
0.006780777	14.77115275	16.851	14.080
0.009473803	12.90087047	15.746	22.054
0.009420783	9.329942433	15.680	68.061
0.012417212	9.668512784	14.497	49.940
0.012399643	9.654832803	14.529	50.484
0.018421514	8.038361653	12.351	53.651
0.019619859	8.236516514	11.970	45.328
0.019602546	8.228494289	11.981	45.604
0.026717953	6.951713624	9.746	40.196
0.026717953	6.954258191	9.746	40.144
0.028282752	5.626175628	9.116	62.028
0.028248737	5.727134246	9.141	59.609
0.033326776	5.981845935	7.940	32.735
0.033326776	5.981299594	7.940	32.747
0.035906956	4.983763621	7.190	44.268
0.036157358	5.019433957	7.128	42.008

Table 12: Literature data and modeling results obtained with ePC-SAFT advanced for the pH of the system water + toluene + acetic acid. *Literature data taken from Ziegenfuß and Maurer[36].

$X_{Acetic\ acid}$ / mol·mol^{-1}	pH$^{exp.,*}$ / -	pH^{Modeled} / -	ARD / %
0.003106633	2.48	2.752	10.968
0.003088565	2.48	2.747	10.766
0.006780777	2.54	2.566	1.0240
0.006780777	2.54	2.569	1.1420
0.009473803	2.54	2.487	2.0870
0.009420783	2.21	2.482	12.308
0.012417212	2.2	2.414	9.7270
0.012399643	2.4	2.415	0.6250
0.018421514	2.03	2.307	13.645
0.019619859	2.31	2.291	0.8230
0.019602546	2.32	2.292	1.2070
0.026717953	2.25	2.201	2.1780
0.026717953	2.24	2.201	1.7410
0.028282752	1.91	2.177	13.979
0.028248737	1.9	2.178	14.632
0.033326776	2.18	2.133	2.1560
0.033326776	2.2	2.133	3.0450
0.035906956	1.84	2.103	14.293
0.036157358	1.83	2.101	14.809

Table 13: Literature data and modeling results of the partition coefficient for the system water + MIBK + oxalic acid.
*Literature data taken from Kirsch and Maurer[37].

$X_{Oxalic\ acid}$ / mol·mol^{-1}	$K^{aq./org.,exp.,*}$ / mol·mol^{-1}	$K^{aq./org.,\ modeled}$ / mol·mol^{-1}	ARD / %
0.002686761	1.522081229	1.478	2.896
0.002668897	1.50159018	1.486	1.038
0.003595687	1.168937551	1.328	13.607
0.003595044	1.160909375	1.326	14.221
0.005464745	1.313488364	1.217	7.346
0.005359124	1.286502542	1.219	5.247
0.005576278	1.225554585	1.202	1.922
0.007452668	1.184448329	1.133	4.344
0.008138001	1.215313327	1.117	8.090
0.00813945	1.218199973	1.117	8.307
0.009087627	1.031242963	1.084	5.116
0.009318322	1.045776464	1.080	3.273
0.010534301	1.18328626	1.070	9.574
0.010551878	1.185260628	1.070	9.724
0.01124288	1.130956715	1.057	6.539
0.012569073	1.16345273	1.047	10.009
0.012569073	1.069677025	1.042	2.587
0.015019026	1.094300104	1.025	6.333
0.019539055	1.032051619	1.014	1.749

Table 14: Literature data and modeling results obtained with ePC-SAFT advanced for the pH of the system water + MIBK + oxalic acid. *Literature data taken from Kirsch and Maurer[37].

$x_{Oxalic\ acid}$ / mol·mol^{-1}	pH$^{exp.,*}$ / -	pH^{Modeled} / -	ARD / %
0.003106633	1.24	1.185	4.435
0.003088565	1.25	1.186	5.120
0.006780777	1.1	1.086	1.273
0.006780777	1.12	1.085	3.125
0.009473803	1.09	0.998	8.440
0.009420783	1.1	1.001	9.000
0.012417212	0.88	0.986	12.045
0.012399643	0.8	0.913	14.125
0.018421514	1	0.895	10.500
0.019619859	1.01	0.896	11.287
0.019602546	0.86	0.851	1.047
0.026717953	0.88	0.847	3.750
0.026717953	0.95	0.832	12.421
0.028282752	0.96	0.831	13.438
0.028248737	0.71	0.811	14.225
0.033326776	0.92	0.788	14.348
0.033326776	0.94	0.778	17.234
0.035906956	0.63	0.738	17.143
0.036157358	0.6	0.667	11.167

Table 15: Literature data and modeling results of the partition coefficient for the system water + MIBK + citric acid. *Literature data taken from Kirsch et al.[17].

$x_{\text{Citric acid}}$ / mol·mol^{-1}	$K^{\text{aq./org.,exp.,*}}$ / mol·mol^{-1}	$K^{\text{aq./org., modeled}}$ / mol·mol^{-1}	ARD / %
0.010741368	14.80704267	14.329	3.228482
0.010758931	14.65979502	12.902	11.99058
0.021505643	13.21644263	11.796	10.74754
0.022612022	14.04712291	10.778	23.27254
0.022612022	13.68030479	10.008	26.84374
0.03610963	12.95023473	9.313	28.08625
0.03626987	12.80374946	8.810	31.19203
0.051300085	11.40020258	8.508	25.36975
0.051300085	11.55690944	8.506	26.39901

Table 16: Literature data and modeling results obtained with ePC-SAFT advanced for the pH of the system water + MIBK + citric acid. *Literature data taken from Kirsch et al.[17].

$x_{\text{Citric acid}}$ / mol·mol^{-1}	$\text{pH}^{\text{exp.,*}}$ / -	$\text{pH}^{\text{Modeled}}$ / -	ARD / %
0.010741368	1.28	1.568	22.500
0.010758931	1.29	1.493	15.736
0.021505643	0.97	1.429	47.320
0.022612022	1.04	1.373	32.019
0.022612022	1.04	1.323	27.212
0.03610963	0.86	1.277	48.488
0.03626987	0.85	1.236	45.412
0.051300085	0.67	1.198	78.806

References

1   M. L. Michelsen, The isothermal flash problem. Part I. Stability, *Fluid Phase Equilibria*, 1982, **9**, 1–19.

2   M. L. Michelsen, The isothermal flash problem. Part II. Phase-split calculation, *Fluid Phase Equilibria*, 1982, **9**, 21–40.

3   W. G. Chapman, K. E. Gubbins, G. Jackson and M. Radosz, SAFT: Equation-of-state solution model for associating fluids, *Fluid Phase Equilibria*, 1989, **52**, 31–38.

4   J. Gross and G. Sadowski, Perturbed-Chain SAFT: An Equation of State Based on a Perturbation Theory for Chain Molecules, *Ind. Eng. Chem. Res.*, 2001, **40**, 1244–1260.

5   L. F. Cameretti, G. Sadowski and J. M. Mollerup, Modeling of Aqueous Electrolyte Solutions with Perturbed-Chain Statistical Associated Fluid Theory, *Ind. Eng. Chem. Res.*, 2005, **44**, 3355–3362.

6   M. Bülow, X. Ji and C. Held, Incorporating a concentration-dependent dielectric constant into ePC-SAFT. An application to binary mixtures containing ionic liquids, *Fluid Phase Equilibria*, 2019, **492**, 26–33.

7   M. Bülow, M. Ascani and C. Held, ePC-SAFT advanced - Part I: Physical meaning of including a concentration-dependent dielectric constant in the born term and in the Debye-Hückel theory, *Fluid Phase Equilibria*, 2021, **535**, 112967.

8   E. Huckel and P. Debye, Zur theorie der elektrolyte. i. gefrierpunktserniedrigung und verwandte erscheinungen, *Phys. Z*, 1923, **24**, 185–206.

9   S. Beret and J. M. Prausnitz, Perturbed hard-chain theory: An equation of state for fluids containing small or large molecules, *AIChE J.*, 1975, **21**, 1123–1132.

10 L. F. Cameretti and G. Sadowski, Modeling of aqueous amino acid and polypeptide solutions with PC-SAFT, *Chemical Engineering and Processing: Process Intensification*, 2008, **47**, 1018–1025.

11 X. Li, C. Peng, J. P. Crawshaw, G. C. Maitland and J. M. Trusler, The pH of CO2-saturated aqueous NaCl and NaHCO3 solutions at temperatures between 308 K and 373 K at pressures up to 15 MPa, *Fluid Phase Equilibria*, 2018, **458**, 253–263.

12 W. Yan, S. Huang and E. H. Stenby, Measurement and modeling of CO2 solubility in NaCl brine and CO2–saturated NaCl brine density, *International Journal of Greenhouse Gas Control*, 2011, **5**, 1460–1477.

13 Y. Liu, M. Hou, G. Yang and B. Han, Solubility of CO2 in aqueous solutions of NaCl, KCl, CaCl2 and their mixed salts at different temperatures and pressures, *The Journal of Supercritical Fluids*, 2011, **56**, 125–129.

14 M. Mutailipu, Y. Liu, Y. Song and J. M. Trusler, The pH of CO2–saturated aqueous KCl solutions at temperatures between 298 K and 423 K at pressures up to 13.5 MPa, *Chemical Engineering Science*, 2021, **234**, 116434.

15 H. Zhao, R. M. Dilmore and S. N. Lvov, Experimental studies and modeling of CO 2 solubility in high temperature aqueous CaCl 2 MgCl 2 Na 2 SO 4 and KCl solutions, *AIChE J.*, 2015, **61**, 2286–2297.

16 S. He and J. W. Morse, The carbonic acid system and calcite solubility in aqueous Na-K-Ca-Mg-Cl-SO4 solutions from 0 to 90°C, *Geochimica et Cosmochimica Acta*, 1993, **57**, 3533–3554.

17 T. Kirsch, H. Ziegenfuß and G. Maurer, Distribution of citric, acetic and oxalic acids between water and organic solutions of tri-n-octylamine, *Fluid Phase Equilibria*, 1997, **129**, 235–266.

18 D. Fuchs, J. Fischer, F. Tumakaka and G. Sadowski, Solubility of Amino Acids: Influence of the pH value and the Addition of Alcoholic Cosolvents on Aqueous Solubility, *Ind. Eng. Chem. Res.*, 2006, **45**, 6578–6584.

19 D. Pabsch, C. Held and G. Sadowski, Modeling the CO 2 Solubility in Aqueous Electrolyte Solutions Using ePC-SAFT, *J. Chem. Eng. Data*, 2020, **65**, 5768–5777.

20 A. Tihic, G. M. Kontogeorgis, N. von Solms and M. L. Michelsen, Applications of the simplified perturbed-chain SAFT equation of state using an extended parameter table, *Fluid Phase Equilibria*, 2006, **248**, 29–43.

21 J. Gross and G. Sadowski, Application of the Perturbed-Chain SAFT Equation of State to Associating Systems, *Ind. Eng. Chem. Res.*, 2002, **41**, 5510–5515.

22 L. Lange, M. Schleinitz and G. Sadowski, Predicting the Effect of pH on Stability and Solubility of Polymorphs, Hydrates, and Cocrystals, *Crystal Growth & Design*, 2016, **16**, 4136–4147.

23 E. A. Crespo, L. P. Silva, M. A. R. Martins, M. Bülow, O. Ferreira, G. Sadowski, C. Held, S. P. Pinho and J. A. P. Coutinho, The role of polyfunctionality in the formation of [ch] cl-carboxylic acid-based deep eutectic solvents, *Ind. Eng. Chem. Res.*, 2018, **57**, 11195–11209.

24 C. Held, T. Reschke, S. Mohammad, A. Luza and G. Sadowski, ePC-SAFT revised, *Chemical Engineering Research and Design*, 2014, **92**, 2884–2897.

25 D. Pabsch, P. Figiel, G. Sadowski and C. Held, Solubility of electrolytes in organic solvents: Solvent-specific effects and ion-specific effects., *Chem. Eng. Data*, 2022.

26 S. Mohammad, C. Held, E. Altuntepe, T. Köse, T. Gerlach, I. Smirnova and G. Sadowski, Salt influence on MIBK/water liquid–liquid equilibrium: Measuring and modeling with ePC-SAFT and COSMO-RS, *Fluid Phase Equilibria*, 2016, **416**, 83–93.

27 A. Roda, F. Santos, Y. Z. Chua, A. Kumar, H. T. Do, A. Paiva, A. R. C. Duarte and C. Held, Unravelling the nature of citric acid:L-arginine:water mixtures: the bifunctional role of water, *Physical chemistry chemical physics : PCCP*, 2021, **23**, 1706–1717.

28 W. M. Haynes, D. R. Lide and T. J. Bruno, *CRC Handbook of Chemistry and Physics*, CRC Press, 2016.

29 F. O. Farias, H. Passos, J. A. P. Coutinho and M. R. Mafra, pH Effect on the Formation of Deep-Eutectic-Solvent-Based Aqueous Two-Phase Systems, *Ind. Eng. Chem. Res.*, 2018, **57**, 16917–16924.

30 D. Li and Z. Duan, The speciation equilibrium coupling with phase equilibrium in the H2O–CO2–NaCl system from 0 to 250 C, from 0 to 1000 bar, and from 0 to 5 molality of NaCl, *Chemical Geology*, 2007, **244**, 730–751.

31 J. Li and Z. Duan, A thermodynamic model for the prediction of phase equilibria and speciation in the H2O–CO2–NaCl–CaCO3–CaSO4 system from 0 to 250 C, 1 to 1000 bar with NaCl concentrations up to halite saturation, *Geochimica et Cosmochimica Acta*, 2011, **75**, 4351–4376.

32 W. B. Floriano and M. A. C. Nascimento, Dielectric constant and density of water as a function of pressure at constant temperature, *Braz. J. Phys.*, 2004, **34**, 38–41.

33 C. Andeen, J. Fontanella and D. Schuele, Low-Frequency Dielectric Constant of LiF, NaF, NaCl, NaBr, KCl, and KBr by the Method of Substitution, *Physical Review B*, 1970, 5068–5073.

34 C. Peng, J. P. Crawshaw, G. C. Maitland, J. P. Martin Trusler and D. Vega-Maza, The pH of CO2-saturated water at temperatures between 308K and 423K at pressures up to 15MPa, *The Journal of Supercritical Fluids*, 2013, **82**, 129–137.

35 X. Han, Z. Yu, J. Qu, T. Qi, W. Guo and G. Zhang, Measurement and Correlation of Solubility Data for CO 2 in NaHCO 3 Aqueous Solution, *J. Chem. Eng. Data*, 2011, **56**, 1213–1219.

36 H. Ziegenfuβ and G. Maurer, Distribution of acetic acid between water and organic solutions of tri-n-octylamine, *Fluid Phase Equilibria*, 1994, **102**, 211–255.

37 T. Kirsch and G. Maurer, Distribution of Oxalic Acid between Water and Organic Solutions of Tri- n -octylamine, *Ind. Eng. Chem. Res.*, 1996, **35**, 1722–1735.